Doubly diversity-induced resonance

Martin Gassel,* Erik Glatt, and Friedemann Kaiser
Institute of Applied Physics, Darmstadt University of Technology, Hochschulstr. 4a, 64289 Darmstadt, Germany
(Received 12 February 2007; published 3 July 2007)

The influence of variability on the response of a net of bistable FitzHugh-Nagumo elements to a weak signal is investigated. The response of the net undergoes a resonancelike behavior due to additive variability. For an intermediate strength of additive variability the external signal is optimally enhanced in the output of the net (*diversity-induced resonance*). Furthermore, we show that additive noise strongly influences the diversity-induced resonance. Afterwards the interplay of additive and multiplicative variability on the response of the net is investigated. Starting with asymmetric bistable elements the enhancement of the signal is not very pronounced in the presence of additive variability. Via symmetry restoration by multiplicative variability the resonance is further enhanced. We call this phenomenon *doubly diversity-induced resonance*, because the interplay of both, additive and multiplicative variability, is essential to achieve the optimal enhancement of the signal. The restoration of symmetry can be explained by a systematic effect of the multiplicative variability, which changes the thresholds for the transitions between the two stable fixed points. We investigate the response to variability for globally and diffusively coupled networks and in dependency on the coupling strength.

DOI: 10.1103/PhysRevE.76.016203 PACS number(s): 05.45.−a, 02.50.−r

It is well known that noise does not always increase disorder, on the contrary it can play a constructive role in many nonlinear systems. Examples are *noise-induced phase transitions*, where the transition is observed at a certain noise strength [1,2], *stochastic resonance*, where the response to an external signal shows a resonancelike behavior due to the noise strength [3], and *coherence resonance* (or *stochastic coherence*), where the output of a nonlinear system is most coherent at a certain noise strength [4]. There are also a lot of examples, where the influence of noise on spatially extended systems is investigated: *Spatiotemporal stochastic resonance*, where the patterns are most coherent or regular due to an intermediate noise strength [5,6]; *array-enhanced coherence resonance* [7], where an array of coupled elements show a significantly stronger coherence compared to that of a single element. *Stochastic resonance* was found in many different physical, chemical, and biological systems [3,8,9]. For instance, the paddle fish takes the advantage of *stochastic resonance* to detect its prey [8]. The constructive role of noise is up to now a topic of great interest. Recently doubly stochastic effects were investigated by Zaikin *et al.* [10,11]. In [11] it is shown that the output signal of a bistable neural element is most coherent at an intermediate strength of additive and multiplicative noise.

Similar to noise, variability (also called diversity [12] or heterogeneity [7]) can crucially influence the spatiotemporal dynamics of a nonlinear system. In contrast to noise, internal variability, which is also omnipresent in nature, denotes static stochastic differences between the otherwise equal elements of a net. The influence of parameter variability on the synchronization of coupled oscillators was investigated by Winfree [13] and Kuramoto [14]. Variability plays an important role for pattern formation in a net of biochemical oscillators [15]. In [16] it was shown that multiplicative variability in a net of coupled FitzHugh-Nagumo (FHN) [17] elements can induce a transition from oscillatory to excitable behavior similar to multiplicative noise [18,19].

Recently, it was shown that variability can induce a resonant collective behavior in a chain of coupled bistable or excitable elements, which are driven by an external signal (*diversity-induced resonance*) [12,20].

In the present paper, the influence of variability and noise on the global response of a net of bistable FHN elements to a weak periodic signal is investigated. We discern additive variability, which denotes variability in an additive parameter of the model equations, and multiplicative variability, which denotes variability in a parameter, that is multiplied to one of the system variables. It is shown that the response of the net exhibits a resonancelike behavior due to additive variability, the external signal is optimally enhanced for an intermediate strength (*diversity-induced resonance*). This effect was first shown by Tessone *et al.* [12] for a globally coupled ensemble of bistable systems and excitable FHN elements. In a very similar manner the optimal enhancement of an external signal is possible in the presence of noise (*stochastic resonance* [3]). We furthermore investigate the interplay of noise and variability, and the influence of the coupling strength on this resonance effect. In a next step the interplay of additive and multiplicative variability is studied for globally and also for diffusively coupled nets. Starting with asymmetric bistable elements (the thresholds for a transition and the inverse transition between the two stable states are unequal) the enhancement of the signal is not very pronounced in the presence of additive variability. Multiplicative variability leads to a restoration of the symmetry (thresholds for the transitions are equal) and the response of the net to the signal is further enhanced compared to the asymmetric case. Since one needs both, additive and multiplicative variability, to achieve the optimal enhancement of the signal, we call this phenomenon *doubly diversity-induced resonance*.

*martin.gassel@physik.tu-darmstadt.de

The system under consideration is a net of $N \times N$ coupled FHN elements, which are driven by a weak periodic signal, in the presence of noise and variability:

$$\frac{du_{ij}}{dt} = \frac{1}{\epsilon}[u_{ij}(1-u_{ij})(u_{ij}-a) - v_{ij} + d] + q_u K_{ij},$$

$$\frac{dv_{ij}}{dt} = u_{ij} - c_{ij} v_{ij} + e_{ij} + \xi_{ij}(t) + A\cos(\omega t). \quad (1)$$

In a neural context, $u_{ij}(t)$ represents the membrane potential of a neuron and $v_{ij}(t)$ is related to the time-dependent conductance of the potassium channels in the membrane [21]. The dynamics of u is much faster than that of v. The separation of the time scales is realized by the small parameter $\epsilon = 0.01$. The time is specified in time units $(t.u.)$. One time unit accords approximately with the limit cycle period of a single FHN element in the oscillatory regime [16]. K_{ij} denotes the coupling function and q_u the coupling strength. A is the amplitude of the external signal and ω its frequency, respectively. The equations are integrated on a discrete spatiotemporal grid using the Heun method ($\Delta t = 0.001$ t.u.) and the forward time centered space scheme in time and space, respectively [2]. The integration in space is performed using periodic boundary conditions. The grid points are labeled by the indices $1 \le i,j \le N$. All simulations are performed with Gaussian distributed random initial conditions.

We consider either global or diffusive coupling between the elements of the net. Global coupling is defined by the coupling function

$$K_{ij} = \langle u_{ij} \rangle_{ij} - u_{ij}, \quad (2)$$

where $\langle u_{ij} \rangle_{ij}$ denotes the spatial mean value of the fast variable of all elements (mean-field coupling). Diffusive, local or nearest-neighbor coupling is implemented using a nine-point discretization of the Laplacian for radial symmetry

$$K_{ij} = \nabla^2 u_{ij},$$

$$\nabla^2 u_{ij} = \frac{1}{6}[u_{i+1,j+1} + u_{i+1,j-1} + u_{i-1,j+1} + u_{i-1,j-1} + 4(u_{i+1,j} + u_{i-1,j} + u_{i,j+1} + u_{i,j-1}) - 20u_{ij}]. \quad (3)$$

In the present contribution only noise and variability in the slow variables $v_{ij}(t)$ are considered. The additive noise term $\xi_{ij}(t)$ is taken to be spatially uncorrelated Gaussian white noise with zero mean. Hence the correlation function reads

$$\langle \xi_{ij}(t)\xi_{kl}(t') \rangle = \sigma_a^2 \delta_{ij,kl} \delta(t-t'), \quad (4)$$

where σ_a denotes the noise strength.

Variability is applied in the parameters e (additive) and c (multiplicative). Both the parameter values e_{ij} and the parameter values c_{ij} are Gaussian distributed numbers with a fixed mean

$$\langle e_{ij} \rangle = E, \quad \langle (e_{ij}-E)(e_{kl}-E) \rangle = \sigma_{va}^2 \delta_{ij,kl}, \quad (5)$$

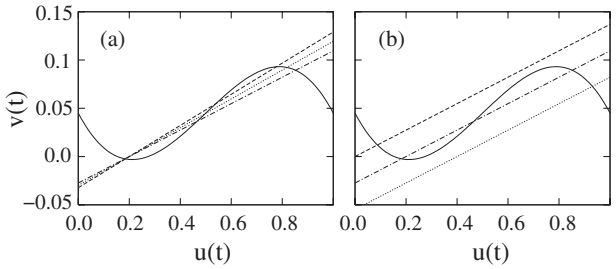

FIG. 1. Nullclines in phase space (u,v) for one FHN element [Eq. (1)]. Cubic nullcline (—). (a) linear nullclines for $e_{ij} = -0.2$ and $c_{ij} = 7.3$ (−·−), $c_{ij} = 6.7$ (···), and $c_{ij} = 6.2$ (−−−). (b) Linear nullclines for $c_{ij} = 7.3$ and $e_{ij} = -0.2$ (−·−), $e_{ij} = -0.4$ (···), and $e_{ij} = 0.0$ (−−−).

$$\langle c_{ij} \rangle = C, \quad \langle (c_{ij}-C)(c_{kl}-C) \rangle = \sigma_{vm}^2 \delta_{ij,kl}. \quad (6)$$

σ_{va} and σ_{vm}, the standard deviation of the Gaussian probability distribution of parameter e $[P(e,\sigma_{va})]$ and c $[P(c,\sigma_{vm})]$, denote the strength of the additive variability and the multiplicative variability, respectively.

Throughout this paper the following set of parameters is used $(a,d,E,N) = (0.5, 0.045, -0.2, 100)$, while parameter C, the coupling strength q_u, the noise strength σ_a, the strength of the additive variability σ_{va}, and the multiplicative variability σ_{vm} are varied.

Without variability all elements of the net are identical. Studying the dynamics of a single uncoupled element (ij element) with parameter $c_{ij} = 7.3$ and $e_{ij} = -0.2$, a stability analyses shows that it is in the bistable regime (two stable foci, which are separated by a saddle point). The parameter c_{ij} determines the slope of the linear nullcline and thereby the thresholds for a transition between the two stable fixed points, which has a crucial influence on the dynamics of the single element. In Fig. 1(a) the nullclines are plotted for different values of parameter c_{ij}. Decreasing the parameter c_{ij} from 7.3 to 6.2 the single element remains in the bistable regime. But the threshold for a transition from the upper to the lower stable fixed point becomes smaller, while the threshold for the inverse transition persists unchanged. For $c_{ij} < 6.1$ the system becomes excitable (only one stable focus, see [16]).

Weak additive noise ($\sigma_a = 0.02$) can induce jumps between the two stable states. In Fig. 2 time series of $u(t)$ of the ij element are shown for three different values of parameter c_{ij}. For $c_{ij} = 7.3$ the system spends roughly all the time in the upper stable fixed point. The threshold for a transition from the upper stable fixed point to the lower stable fixed point is larger than the threshold for the inverse transition. This case is called the asymmetric bistable regime throughout this paper. For $c_{ij} = 6.7$ the system spends roughly the same time in both stable states. So the thresholds for transitions between the two stable fixed points are approximately of the same size (symmetric bistable regime). For $c_{ij} = 6.2$ the threshold for a transition from the upper stable fixed point to the lower stable fixed point is smaller than the threshold for the inverse transition, the system prefers to stay in the lower state.

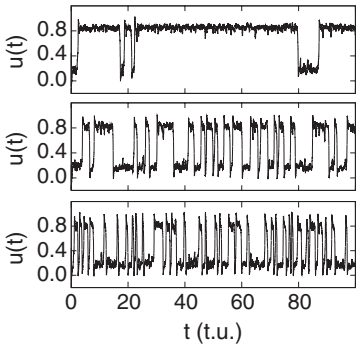

FIG. 2. Time series of $u(t)$ of a single uncoupled FHN element for different parameters c_{ij} (from bottom to top: $c_{ij}=6.2,6.7,7.3$) driven by weak additive noise $\sigma_a=0.02$; without external signal.

In presence of variability the net is a mixture of FHN elements in different dynamical regimes. The parameter values c_{ij} differ from element to element as described above [Eq. (6)] with the fixed mean $C=7.3$ [Fig. 3(a)]. For $c_{ij}<0$ the slope of the linear nullcline is negative and the dynamics of the element changes completely. Consequently these parameter values have to be excluded by setting the probability distribution $P(c,\sigma_{vm})$ equal to zero for $c<0$. For $\sigma_{vm}=3.5$, the largest variability strength used in this paper, less than 2% of the Gaussian distributed c_{ij} are excluded. The mean and the variance of the cutoff Gaussian distribution slightly differ from the predetermined values C and σ_{vm}, respectively, but that has no considerable effect on the presented results. Using a symmetric cutoff of the Gaussian distribution one gets even quantitatively the same results.

We follow reference [16] to estimate the deterministic influence of the multiplicative variability on the dynamics of the net. There it is shown that the mean gradient angle of the linear nullclines of all elements is a macroscopic net parameter that explains the global dynamics of large nets with sufficiently strong coupling. The mean angle is given by

$$\langle\alpha\rangle = \langle\alpha_{ij}\rangle_{ij} = \frac{1}{N^2}\sum_{i,j=1}^{N}\left[\arctan\left(\frac{1}{c_{ij}}\right)\right] \tag{7}$$

and gets systematically changed by the strength of the multiplicative variability. It can be calculated approximately for a large net as

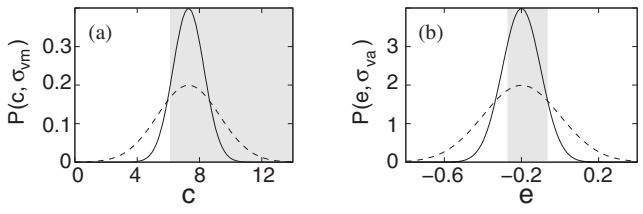

FIG. 3. (a) Gaussian probability distribution $P(c,\sigma_{vm})$ in dependency on c for $\sigma_{vm}=1.0$ (—) and $\sigma_{vm}=2.0$ (– – –), $C=7.3$, $E=-0.2$, $\sigma_{va}=0.0$. (b) Gaussian probability distribution $P(e,\sigma_{va})$ in dependency on e for $\sigma_{va}=0.1$ (—) and $\sigma_{va}=0.2$ (– – –), $E=-0.2$, $C=7.3$, $\sigma_{vm}=0.0$. The gray area marks the bistable regime, the white areas the excitable regimes.

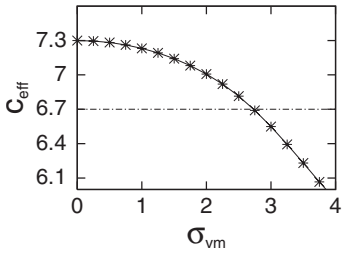

FIG. 4. Deterministic influence of the multiplicative variability: The systematic change of the effective parameter c_{eff} dependent on the strength of multiplicative variability σ_{vm}. (–·–) corresponds to the symmetric case $C=6.7$.

$$\langle\alpha\rangle \approx \int_{-\infty}^{\infty}\arctan\left(\frac{1}{c}\right)P(c,\sigma_{vm})dc. \tag{8}$$

In Fig. 4 this theoretical estimation is plotted dependent on σ_{vm} introducing an effective parameter c_{eff}

$$c_{\text{eff}} := \frac{1}{\tan(\langle\alpha\rangle)}. \tag{9}$$

The effective parameter c_{eff} decreases with an increasing strength of the multiplicative variability σ_{vm}. So the averaged slope of the linear nullcline of all elements becomes steeper with an increase of σ_{vm} and the mean threshold (threshold averaged over all elements) for a transition from the upper to the lower stable fixed point becomes smaller.

The parameter e_{ij} determines the position of the linear nullcline regarding the v axis [Fig. 1(b)] and thereby the thresholds for a transition between the two stable fixed points. For $e_{ij}>-0.07(e_{ij}<-0.27)$ and $c_{ij}=7.3$ the single uncoupled element becomes excitable, only one stable focus at the left (right) branch of the cubic nullcline exists. But due to coupling the network shows bistable dynamics at least for those values of additive and multiplicative variability, which are applied in the simulations presented in this paper.

Now the external signal with amplitude $A=0.04$ and frequency $\omega=0.6$ t.u.$^{-1}$ is switched on to investigate the influence of variability on the response of the net to the signal. For the given set of parameters and without variability the signal cannot induce jumps between the two stable states. The net remains in one of the fixed points. To quantify the response of the net to the signal the linear response Q, the Fourier transform of the mean-field time series $\langle u_{ij}(t)\rangle_{ij}$ at the fixed driver frequency ω, scaled on the amplitude A is used

$$Q = \frac{\omega}{2n\pi A}\left|\int_0^{2n\pi/\omega} 2\langle u_{ij}(t)\rangle_{ij}e^{(i\omega t)}dt\right|. \tag{10}$$

First the influence of both, additive variability and noise, on the response of the net is investigated. In Fig. 5 the linear response Q of a globally coupled net is plotted in dependency on σ_{va} and σ_a. In this simulation the elements are in the symmetric bistable regime ($C=6.7$; $\sigma_{vm}=0.0$). The linear response Q shows a resonancelike behavior due to both, additive variability and noise. Without noise ($\sigma_a=0.0$) the signal is optimally enhanced for an intermediate strength of σ_{va}

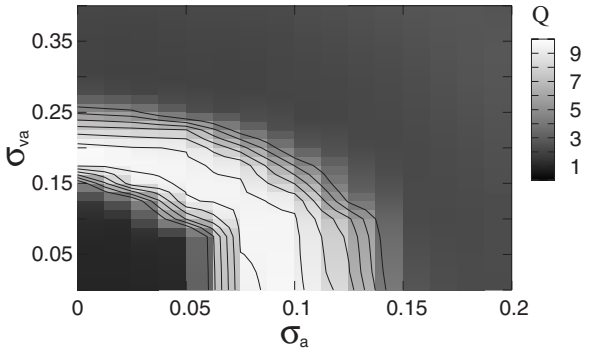

FIG. 5. Linear response Q of a globally coupled net dependent on the strength of additive variability and noise. $q_u=20$; $\sigma_{vm}=0.0$; $C=6.7$ (symmetric case). Contour lines from the outside to the inside: 4.5; 5.5; 6.5; 7.5; 8.5; 9.5.

(*diversity-induced resonance* [12]). Without variability ($\sigma_{va}=0.0$) the system shows the well-known phenomenon of *stochastic resonance*, where the optimal signal enhancement is reached at intermediate noise strengths σ_a [3]. The symmetry of the linear response with respect to σ_{va} and σ_a is exhibited in Fig. 5 and shows that one can replace additive noise by additive variability. The more noise is present, the less variability is necessary to achieve optimal signal enhancement and vice versa.

Without additive noise the temporal evolution of the net is deterministic. Additive variability causes a shift of the linear nullcline for each element up or down [Fig. 1(b)]. The distribution of parameter e_{ij} is shown in Fig. 3(b). For $\sigma_{va}>0$ there are bistable elements, which are driven beyond the threshold of one of its fixed points by the external signal, and even excitable elements. These elements would switch to the other stable state and to their only stable state, respectively, if they were uncoupled. In Fig. 6 mean-field time series of u are plotted for different values of σ_{va}. For a small variability strength (e.g., $\sigma_{va}=0.1$) the signal cannot induce jumps between the two stable states for most of the elements. So due to coupling the net is bound to one of the two stable fixed

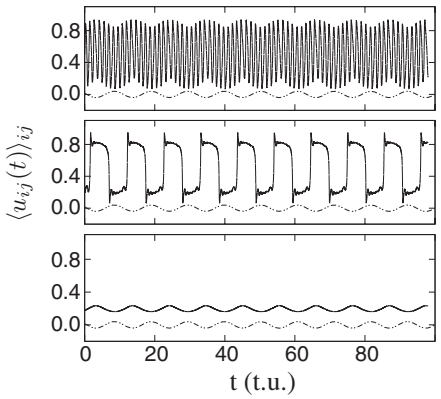

FIG. 6. Time series of the mean field $\langle u_{ij}(t)\rangle_{ij}$ of a globally coupled net for different parameter values of σ_{va} (from bottom to top: $\sigma_{va}=0.1, 0.2, 0.3$). (···) the external signal; (—) $\langle u_{ij}(t)\rangle_{ij}$; $q_u=20$; $\sigma_a=0.0$; $\sigma_{vm}=0.0$; $C=6.7$.

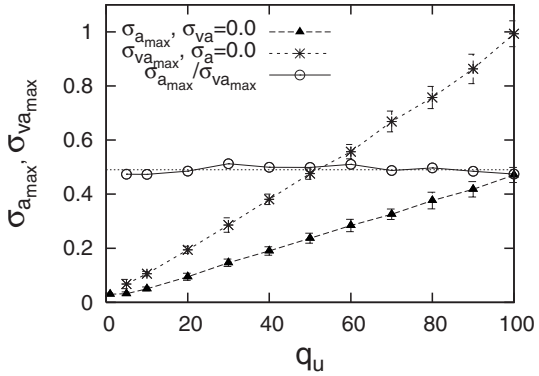

FIG. 7. $\sigma_{va_{max}}$, $\sigma_{a_{max}}$ and their quotient dependent on q_u. Additionally the mean value of the quotients $\langle\sigma_{a_{max}}/\sigma_{va_{max}}\rangle=0.49$ is plotted as reference line (···).

points. Increasing the variability strength σ_{va}, more and more elements can switch to the other stable state at a certain phase of the external signal. These elements pull the others producing a collective behavior. The whole net is performing jumps between the two stable states synchronized to the external forcing (Fig. 6, $\sigma_{va}=0.2$). For an even larger variability strength (e.g., $\sigma_{va}=0.3$) the net permanently jumps between the two stable states, like a synchronized oscillation, but independent of the external forcing. The signal is not enhanced in the response of the net anymore. The permanent jumps of the net between the two stable states can also be observed without an external signal at a certain level of additive variability or noise. For a very large variability strength the collective behavior gets more and more lost. This result confirms that the phenomenon of *diversity-induced resonance* is generic, as proposed by Tessone *et al.* [12].

The corresponding mean-field time series of u dependent on σ_a without variability show pretty much the same behavior as those in Fig. 6 (not printed here). Replacing additive noise by additive variability leads in this case to a very similar collective behavior.

The observed resonance strongly depends on the coupling strength. We denote the value of σ_{va} for $\sigma_a=0.0$ and σ_a for $\sigma_{va}=0.0$, at which Q takes its maximum, as $\sigma_{va_{max}}$ and $\sigma_{a_{max}}$, respectively. Both $\sigma_{va_{max}}$ and $\sigma_{a_{max}}$ linearly depend on the coupling strength over a wide range of q_u (Fig. 7). Their quotient is approximately a constant ($\sigma_{a_{max}}/\sigma_{va_{max}}\approx 0.49$). So one needs roughly twice as much strength of additive variability than strength of additive noise to get optimal signal enhancement for the investigated range of q_u. For vanishing coupling strength $\sigma_{a_{max}}$ tends to 0.03, the value one gets for a single uncoupled element. Regarding additive variability the response of the net shows no resonance for $q_u<5$. So a minimum coupling strength is essential to obtain diversity-induced resonance.

Now the combined influence of multiplicative variability and additive variability on the response of the net to the signal is investigated. The simulations are performed without additive noise starting in the asymmetric bistable regime ($C=7.3$). In Fig. 8 the linear response of a globally coupled net is shown in dependency on σ_{va} and σ_{vm}. The additive

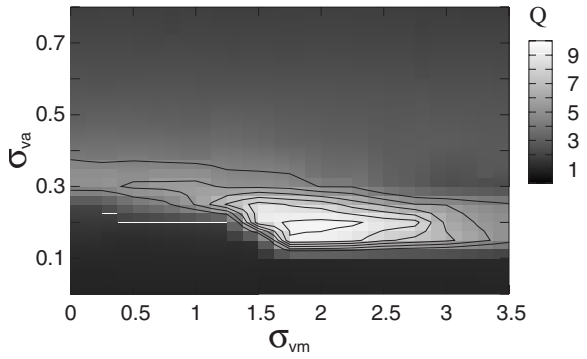

FIG. 8. Linear response Q of a globally coupled net dependent on the strength of additive and multiplicative variability. $q_u=20$; $\sigma_a=0.0$; $C=7.3$. Contour lines as in Fig. 5.

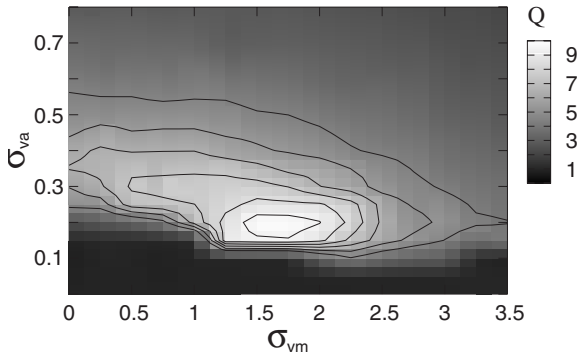

FIG. 10. Linear response Q of a diffusively coupled net dependent on the strength of additive and multiplicative variability. $q_u=20$; $\sigma_a=0.0$; $C=7.3$. Contour lines as in Fig. 5.

variability is responsible for the synchronized hopping between the two stable states. This also works in the asymmetric case ($C=7.3$ and $\sigma_{vm}=0.0$), but the maximum of Q is shifted to larger values of σ_{va} and it is less pronounced.

Applying additionally multiplicative variability the maximum is reached for smaller values of σ_{va} and becomes higher. For an optimal value of $\sigma_{vm}\approx 2.0$ the linear response curve takes its absolute maximum value. For even larger values of σ_{vm} the maximum of the resonance curve decreases again. The multiplicative variability changes the mean threshold for a transition from the upper to the lower stable fixed point. Using the theoretical estimation for the influence of multiplicative variability the optimal value $\sigma_{vm}=2.0$ corresponds to $c_{\text{eff}}\approx 7.0$ (Fig. 4), which shows that the system is shifted towards the symmetric bistable regime $C=6.7$. The quantitative agreement is even better for larger nets with stronger coupling. So via symmetry restoration by multiplicative variability the response of the net to the signal is further enhanced. We call this effect *doubly diversity-induced resonance*, because both, additive and multiplicative variability, are necessary to enhance the external signal optimally.

In Fig. 9 mean-field time series of u are plotted for particular values of σ_{va} and σ_{vm} to manifest this result. In each column (different fixed values of σ_{vm}) one sees that the additive variability is responsible for the synchronized hopping between the two stable states, as described above for the symmetric bistable regime. The strength of additive variability, at which this synchronized hopping occurs, depends on the value of σ_{vm}. The constructive influence of the multiplicative variability causes a modification of the mean thresholds for the transitions between the two stable fixed points. Comparing the time series for $\sigma_{va}=0.2$ of Fig. 9 one sees that for $\sigma_{vm}=2.0$ the symmetry is restored, the thresholds for a transition and the inverse transition between the two stable states are approximately of the same size. The net spends the same time in both stable states.

In Figs. 10 and 11, respectively, the results of the simulations of diffusively coupled nets are shown. The linear response Q shows again a well-pronounced maximum (Fig.

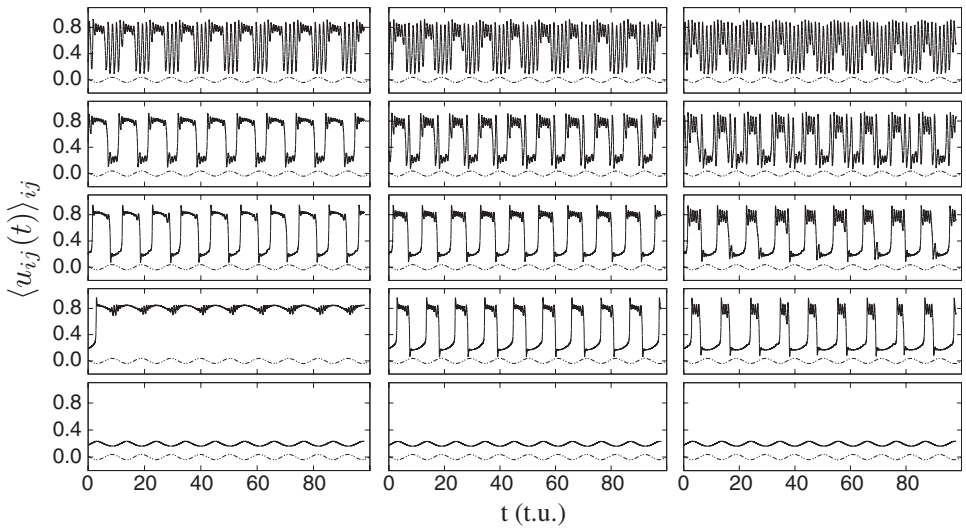

FIG. 9. Time series of the mean field $\langle u_{ij}(t)\rangle_{ij}$ of a globally coupled net for different parameter values of σ_{va} and σ_{vm}. Left column: $\sigma_{vm}=1.5$. Middle column: $\sigma_{vm}=2.0$. Right column: $\sigma_{vm}=2.5$. In each column from bottom to top: $\sigma_{va}=0.1, 0.15, 0.2, 0.25, 0.3$. (···) the external signal; (—) $\langle u_{ij}(t)\rangle_{ij}$; $q_u=20$; $\sigma_a=0.0$; $C=7.3$.

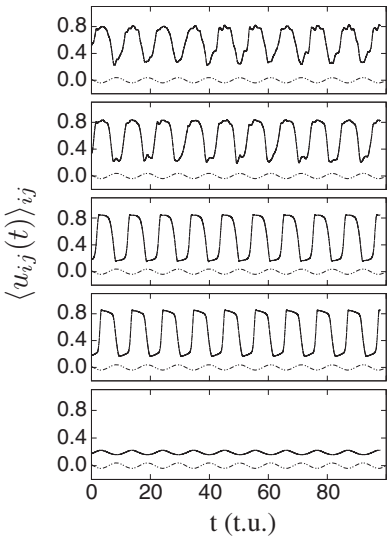

FIG. 11. Time series of the mean field $\langle u_{ij}(t)\rangle_{ij}$ of a diffusively coupled net for different parameter values of σ_{va} (from bottom to top: σ_{va}=0.1,0.15,0.2,0.25,0.3). (···) the external signal; (—) $\langle u_{ij}(t)\rangle_{ij}$; q_u=20; σ_{vm}=1.75; σ_a=0.0; C=7.3.

10) in dependency on σ_{va} and σ_{vm}. In comparison to the globally coupled case the optimal signal enhancement is reached for slightly smaller values of the multiplicative variability σ_{vm}. Regarding the influence of additive variability the optimal signal enhancement occurs approximately at the same value of σ_{va} compared to the globally coupled case, but the decrease of Q is stretched over a larger range of σ_{va}. In Fig. 11 mean-field time series of u are shown for particular values of σ_{va} and for the optimal value of σ_{vm}=1.75. Analogous to the results of the globally coupled net, the additive variability is responsible for the synchronized hopping between the two stable states and the multiplicative variability restores the symmetry. In a diffusively coupled net the elements, which can switch to the other stable state at a certain phase of the signal, pull the nearest-neighbor elements to the other stable state. So a jump from one stable state to the other one propagates like a phase wave through the whole net in contrast to the globally coupled net. That is the reason why the mean-field time series are smoother compared to the globally coupled case.

An obvious difference to the globally coupled case is that an increase of the strength of additive variability beyond the optimal value does not induce the oscillationlike permanent hopping between the two stable states. The global coupling forces all elements to act synchronously and leads thereby to the oscillationlike permanent hopping, which is responsible for the fast decrease of Q at large values of σ_{va}. The diffusive local coupling can not force all elements to act synchronously at large values of σ_{va}, only ever smaller clusters jump synchronously. That is the reason, why the collective behavior monotonously disappears with higher values of σ_{va}. The amplitude of the mean-field time series gets smaller, and the external signal becomes less and less enhanced in the response of the net over a wide range of σ_{va}.

The maximum values of the response Q are approximately the same for the globally (Fig. 8) and the locally (Fig. 10) coupled net. The amplitude of the response of the net is determined by the positions of the two stable states, which is the same in both cases independent of the type of coupling. For local coupling a jump from one stable state to the other, which propagates like a phase wave through the net, takes indeed a bit more time than for global coupling. But due to the sufficiently large coupling strength this time is very short compared to the period of the signal. For that reason there is no noticeable difference between the maximum values of the response of the globally and the locally coupled net. In comparison to the maximum value of the response of the net in the symmetric bistable regime (Fig. 5) one sees again no considerable difference. That means that the symmetry is restored by the multiplicative variability without adverse effects on the net dynamics.

In conclusion, we have shown that an external signal can optimally be enhanced in the output of a net of bistable FHN elements, if a certain strength of additive variability is applied. The response of the net to the signal exhibits a resonancelike behavior in dependency on the strength of the additive variability (diversity-induced resonance). This result manifests the generic constitution of *diversity-induced resonance*, as proposed by Tessone *et al.* [12]. We have furthermore shown that additive noise strongly influences the diversity-induced resonance. The more noise is present, the less variability is necessary to achieve the optimal enhancement of the signal. The variability strength, at which the signal is optimally enhanced, linearly depends on the coupling strength over a wide range. However the coupling strength must exceed a certain value to obtain this resonancelike behavior.

In the second part of our paper we have investigated the interplay of additive and multiplicative variability for globally and also for diffusively coupled nets. Starting with asymmetric bistable elements the resonance is not very pronounced in the presence of additive variability. But this resonance can further be enhanced via a restoration of the symmetry by multiplicative variability (doubly diversity-induced resonance). The interplay of additive and multiplicative variability is essential to achieve the optimal enhancement of the signal. A theoretical estimation of the systematic influence of multiplicative variability on the network dynamics is given, which explains quite well the results of the numerical simulations.

The presented results underline that variability can have a constructive influence on the dynamics of spatially extended nonlinear systems. Especially the interaction of different sources of variability and noise might have a crucial impact on the dynamics of complex systems. The resonancelike response on a signal due to additive and multiplicative variability is studied using the paradigmatic FHN model in a rather general framework. We believe that the interplay of different sources of variability can play a constructive role in many other nonlinear systems. There might be many applications in several fields of physics, neuroscience, and biology, where variability may improve signal detection. We hope that our investigations will contribute to the theory of extended systems under the influence of variability and noise and that the results can be verified in an experimental work.

[1] C. Van den Broeck, J. M. R. Parrondo, and R. Toral, Phys. Rev. Lett. **73**, 3395 (1994).
[2] J. García-Ojalvo and J. M. Sancho, *Noise in Spatially Extended Systems* (Springer, Berlin, 1999).
[3] L. Gammaitoni, P. Hänggi, P. Jung, and F. Marchesoni, Rev. Mod. Phys. **70**, 223 (1998).
[4] A. S. Pikovski and J. Kurths, Phys. Rev. Lett. **78**, 775 (1997).
[5] P. Jung and G. Mayer-Kress, Phys. Rev. Lett. **74**, 2130 (1995).
[6] H. Busch and F. Kaiser, Phys. Rev. E **67**, 041105 (2003).
[7] C. Zhou, J. Kurths, and B. Hu, Phys. Rev. Lett. **87**, 098101 (2001).
[8] D. F. Russell, L. A. Wilkens, and F. Moss, Nature (London) **402**, 291 (1999).
[9] B. Lindner, J. García-Ojalvo, A. Neiman, and L. Schimansky-Geier, Phys. Rep. **392**, 321 (2004).
[10] A. A. Zaikin, J. Kurths, and L. Schimansky-Geier, Phys. Rev. Lett. **85**, 227 (2000).
[11] A. Zaikin, J. García-Ojalvo, R. Bascones, E. Ullner, and J. Kurths, Phys. Rev. Lett. **90**, 030601 (2003).
[12] C. J. Tessone, C. R. Mirasso, R. Toral, and J. D. Gunton, Phys. Rev. Lett. **97**, 194101 (2006).
[13] A. T. Winfree, J. Theor. Biol. **16**, 15 (1967).
[14] Y. Kuramoto, *Chemical Oscillations, Waves and Turbulence* (Springer, Berlin, 1984).
[15] M.-T. Hütt, H. Busch, and F. Kaiser, Nova Acta Leopold. **332**, 381 (2003).
[16] E. Glatt, M. Gassel, and F. Kaiser, Phys. Rev. E **73**, 066230 (2006).
[17] J. S. Nagumo and S. Yoshizawa, Proc. IRE **50**, 2061 (1962).
[18] E. Ullner, A. Zaikin, J. García-Ojalvo, and J. Kurths, Phys. Rev. Lett. **91**, 180601 (2003).
[19] E. Glatt, H. Busch, F. Kaiser, and A. Zaikin, Phys. Rev. E **73**, 026216 (2006).
[20] R. Toral, C. J. Tessone, and J. V. Lopes, Eur. Phys. J. - Special Topics **143**, 59 (2007).
[21] J. Keener and J. Snyder, *Mathematical Physiology* (Springer, New York, 1998).